Surface Complexation Modeling[☆]

S Goldberg, USDA-ARS U.S. Salinity Laboratory, Riverside, CA, USA

Symbols

$(\sigma_{\log K})_I$	Standard deviation for logK of the Ith data set
a	Particle concentration [g l^{-1}]
A^-	Anion of the background electrolyte
C	Capacitance [F m^{-2}]
C^+	Cation of the background electrolyte
C_1	Capacitance between the o- and the β-plane [F m^{-2}]
C_2	Capacitance between the β- and the d-plane [F m^{-2}]
D	Dielectric constant of water
F	Faraday constant [C mol^{-1}]
I	Ionic strength
K_I	Equilibrium constant
L	Ligand
l^{l-}	Charge on the ligand
M	Metal ion
m^{m+}	Charge on the metal
N_A	Avogadro's number
N_S	Maximum surface site density [sites nm^{-2}]
R	Molar gas constant [J mol^{-1} K^{-1}]
S	Surface area [m^2 g^{-1}]
SOH	Reactive surface hydroxyls bound to a metal ion S
S_s	High-affinity sites
S_T	Total number of reactive surface functional groups
S_w	Low-affinity sites
T	Absolute temperature [K]
ϵ_o	Permittivity of vacuum [C^2 J^{-1} m^{-1}]
σ	Surface charge density [C m^{-2}]
σ_d	Surface charge density in the d-plane [C m^{-2}]
σ_o	Surface charge density in the o-plane [C m^{-2}]
σ_β	Surface charge density in the β-plane [C m^{-2}]
Ψ	Surface potential [V]
Ψ_d	Surface potential in the d-plane [V]
Ψ_o	Surface potential in the o-plane [V]
Ψ_β	Surface potential in the β-plane [V]

Introduction

Adsorption is the process through which ions are removed from solution and accumulate at a solid surface. The ion accumulation takes place at the interface between the surface and the solution forming a two-dimensional structure. If adsorption continues and leads to a three-dimensional structure, the process is called precipitation. The general loss of ions from solution to a surface is called sorption.

Adsorption can occur either specifically or non-specifically. Specific adsorption occurs when ions have a high affinity for the surface and it results in the formation of inner-sphere surface complexes. Inner-sphere surface complexes are complexes that contain no water molecules between the adsorbing ion and the surface functional group. Examples of surface functional groups are

---

[☆] *Change History:* May 2013. S Goldberg updated the Sections: Surface Configuration of the Solid-Solution Interface, Mass and Charge Balances, Charge-Potential Relationships, Constant Capacitance Model, Diffuse-Layer Model, Triple-Layer Model, One-pK Model, and Further Reading.

http://dx.doi.org/10.1016/B978-0-12-409548-9.05311-2

reactive hydroxyl groups on oxide or clay minerals and carboxyl or phenol groups on organic matter. Such surface functional groups are a source of solid surface charge since they undergo dissociation and/or protonation reactions as a result of changes in solution pH. Specific anion adsorption occurs via ligand exchange where the adsorbing ion replaces a reactive surface hydroxyl from the surface functional group. Nonspecific adsorption is dominated by electrostatic attraction and results in outer-sphere complex formation or in adsorption in the diffuse ion swarm. Adsorption in the diffuse ion swarm is the weakest type of adsorption since the ion does not attach to a specific surface functional group but remains free in the aqueous solution, neutralizing surface charge only by its proximity to the charged solid surface. Outer-sphere surface complexes are also formed through nonspecific adsorption and contain at least one water molecule between the adsorbing ion and the surface functional group.

A model is a simplified representation of reality that considers only those characteristics of the system that are pertinent to the problem at hand. A chemical model provides a description of a chemical system consistent with its chemical properties while simultaneously being as simple and as chemically correct as possible. The ideal chemical model is realistic, effective, comprehensive, and predictive. A realistic model conforms to accepted theories of chemical behavior, an effective model closely describes experimental observations, a comprehensive model applies to a wide range of experimental conditions without modification, and a predictive model can be applied to various different chemical conditions.

Description of Models

Surface complexation models are chemical models that give a molecular description of adsorption phenomena using an equilibrium approach. Analogous to complex formation in solution, surface complexation models define surface species, chemical reactions, equilibrium constants, mass balances, and charge balances and their molecular features can be given thermodynamic significance. One of the major advancements of surface complexation models is consideration of the charge on both the adsorbing ion and the solid adsorbent surface. Surface complexation models constitute a family of models having many common characteristics and adjustable parameters. The models differ in their structural representation of the solid–solution interface, i.e., the location and surface configuration of the adsorbed ions.

Surface Configuration of the Solid–Solution Interface

Members of the surface complexation model family include the two-pK models: constant capacitance, diffuse-layer, triple-layer. Two-pK models are based on a reactive surface functional group, SOH, that undergoes both protonation and dissociation:

$$\mathrm{SOH} + \mathrm{H}^+ \leftrightarrow \mathrm{SOH}_2^+ \qquad [1]$$

$$\mathrm{SOH} \leftrightarrow \mathrm{SO}^- + \mathrm{H}^+ \qquad [2]$$

hence the term two-pK model.

Comparable models can be written based on the one-pK concept. The one-pK model was originally developed based on the Stern model. In the one-pK model, surface functional groups carry either one or two protons, SOH and $\mathrm{SOH_2}$, respectively. Surface charging can be represented with one reaction:

$$\mathrm{SOH}^{1/2-} + \mathrm{H}^+ \leftrightarrow \mathrm{SOH}_2^{1/2+} \qquad [3]$$

The location and surface configuration of the adsorbed ions for the various surface complexation models are presented in Figure 1. In the constant capacitance model and the diffuse layer model all surface complexes are inner-sphere and are located in a single surface plane (Figure 1(a), 1(b)). The diffuse-layer model includes a diffuse layer that commences at the d-plane and extends into solution. In the triple-layer model ions forming inner-sphere surface complexes adsorb in the surface o-plane and ions forming outer-sphere surface complexes adsorb in a β-plane located between the o-plane and the d-plane (Figure 1(c)). In the representation of the one-pK model based on the Stern model indicated in Figure 1(d), protons and hydroxyls form inner-sphere surface complexes located in the o-plane; all other ions form outer-sphere surface complexes and are located in the d-plane. Subsequent expansions of the one-pK model resulted in the charge distribution multisite complexation (CD-MUSIC) model which uses the charge distribution and bond valence principles and identifies surface sites based on their crystallographic structure.

Surface Complexation Reactions

In the two-pK models chemical reactions for inner-sphere surface complexation are [1] and [2], and:

$$\mathrm{SOH} + \mathrm{M}^{m+} \leftrightarrow \mathrm{SOM}^{(m-1)} + \mathrm{H}^+ \qquad [4]$$

$$2\mathrm{SOH} + \mathrm{M}^{m+} \leftrightarrow (\mathrm{SO})_2\mathrm{M}^{(m-2)} + 2\mathrm{H}^+ \qquad [5]$$

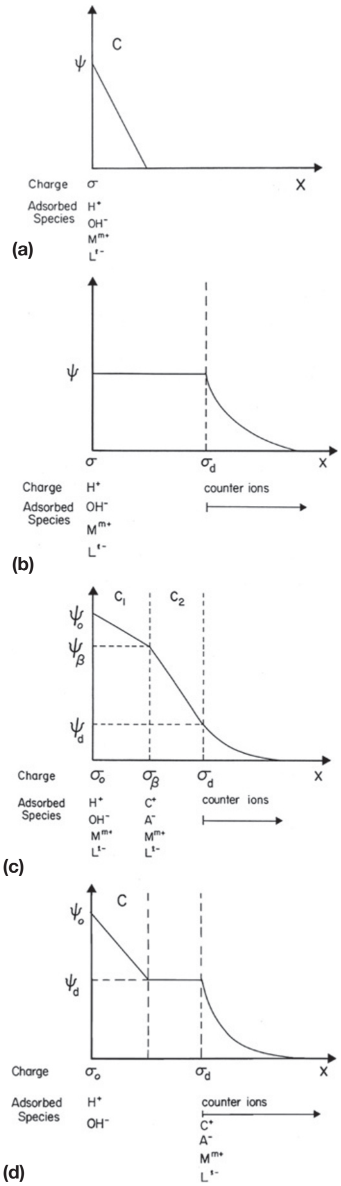

Figure 1 Placement of ions, potentials, charges, and capacitances for the (a) constant capacitance model (after Westall, (1986)); (b) diffuse layer model, (after Dzombak and Morel (1990)); (c) triple layer model, (after Westall, (1980)); (d) one-pK model, (after Westall, (1986)). (a) and (d) Reproduced from Davis JA and Hayes K (eds) *Geochemical Processes at Mineral Surfaces*, ACS symposium Series 323: 54–78, Copyright (1986) American Chemical Society; (b) reprinted from Dzombak, D.A. and Morel, F.M.M. (1990). *Surface Complexation Modeling. Hydrous Ferric Oxide*. New York: Wiley, with permission from Wiley; (c) reprinted with permission from Kavanaugh, M.C. and Leckie, J.O. (eds) *Particulates in Water Characterization*, *Fate*, *Effects and Removal*. ACS Advances in Chemistry Series 189: 33–44, Copyright (1980) American Chemical Society.

$$\mathrm{SOH} + \mathrm{L}^{1-} + \mathrm{H}^{+} \leftrightarrow \mathrm{SL}^{(1-1)-} + \mathrm{H_2O} \qquad [6]$$

$$2\mathrm{SOH} + \mathrm{L}^{1-} + 2\mathrm{H}^{+} \leftrightarrow \mathrm{S_2L}^{(1-2)} + 2\mathrm{H_2O} \qquad [7]$$

$$\mathrm{SOH} + \mathrm{L}^{1-} + 2\mathrm{H}^{+} \leftrightarrow \mathrm{SHL}^{(1-2)} + \mathrm{H_2O} \qquad [8]$$

where M is a metal ion of charge m^+ and L is a ligand of charge l^-. Surface complexes can be monodentate or bidentate. In monodentate complexation one bond is formed between the adsorbing ion and the surface functional group. Bidentate complexes contain two bonds between the adsorbing ion and two surface functional groups. Equations [4]–[7] are used in the constant capacitance model. In the diffuse-layer model, reaction [8] is used in place of reaction [7] since bidentate complexes for adsorbed anions have not been considered.

The following chemical reactions for outer-sphere surface complexation are considered in the triple-layer model in addition to [1], [2], [4]–[7]:

$$\mathrm{SOH + M^{m+} \leftrightarrow SO^- - M^{m+} + H^+} \qquad [9]$$

$$\mathrm{SOH + M^{m+} + H_2O \leftrightarrow SO^- - MOH^{(m-1)} + 2H^+} \qquad [10]$$

$$\mathrm{SOH + H^+ + L^{1-} \leftrightarrow SOH_2^+ - L^{1-}} \qquad [11]$$

$$\mathrm{SOH + 2H^+ + L^{1-} \leftrightarrow SOH_2^+ - LH^{(1-1)-}} \qquad [12]$$

$$\mathrm{SOH + C^+ \leftrightarrow SO^- - C^+ + H^+} \qquad [13]$$

$$\mathrm{SOH + H^+ + A^- \leftrightarrow SOH_2^+ - A^-} \qquad [14]$$

where C^+ is the cation and A^- is the anion of the background electrolyte.

In the one-pK models, chemical reactions for surface complexation are eqn [3] and:

$$\mathrm{SOH^{1/2-} + M^{m+} \leftrightarrow SOH^{1/2-} - M^{m+}} \qquad [15]$$

$$\mathrm{SOH^{1/2-} + M^{m+} + H_2O \leftrightarrow SOH^{1/2-} - MOH^{(\mathit{m}-1)} + H^+} \qquad [16]$$

$$\mathrm{SOH_2^{1/2+} + L^{1-} \leftrightarrow SOH_2^{1/2+} - L^{1-}} \qquad [17]$$

$$\mathrm{SOH^{1/2-} + C^+ \leftrightarrow SOH^{1/2-} - C^+} \qquad [18]$$

$$\mathrm{SOH_2^{1/2+} + A^- \leftrightarrow SOH_2^{1/2+} - A^-} \qquad [19]$$

Equilibrium Constants for Surface Complexation

The equilibrium constants describing inner-sphere surface complexation in the two-pK models are:

$$K_+ = \frac{[\mathrm{SOH_2^+}]}{[\mathrm{SOH}][\mathrm{H^+}]} \exp\left[\mathrm{F}\Psi/RT\right] \qquad [20]$$

$$K_- = \frac{[\mathrm{SO^-}][\mathrm{H^+}]}{[\mathrm{SOH}]} \exp\left[-\mathrm{F}\Psi/RT\right] \qquad [21]$$

$$K_\mathrm{M}^1 = \frac{\left[\mathrm{SOM^{(m-1)}}\right][\mathrm{H^+}]}{[\mathrm{SOH}][\mathrm{M^{m+}}]} \exp\left[(\mathrm{m}-1)\mathrm{F}\Psi/RT\right] \qquad [22]$$

$$K_\mathrm{M}^2 = \frac{\left[\mathrm{(SO)_2M^{(m-2)}}\right][\mathrm{H^+}]^2}{[\mathrm{SOH}]^2[\mathrm{M^{m+}}]} \exp\left[(\mathrm{m}-2)\mathrm{F}\Psi/RT\right] \qquad [23]$$

$$K_\mathrm{L}^1 = \frac{\left[\mathrm{SL^{(1-1)-}}\right]}{[\mathrm{SOH}]\left[\mathrm{L^{1-}}\right][\mathrm{H^+}]} \exp\left[-(1-1)\mathrm{F}\Psi/RT\right] \qquad [24]$$

$$K_\mathrm{L}^2 = \frac{\left[\mathrm{S_2L^{(1-2)-}}\right]}{[\mathrm{SOH}]^2\left[\mathrm{L^{1-}}\right][\mathrm{H^+}]^2} \exp\left[-(1-2)\mathrm{F}\Psi/RT\right] \qquad [25]$$

$$K_\mathrm{L}^3 = \frac{\left[\mathrm{SHL^{(1-2)-}}\right]}{[\mathrm{SOH}]\left[\mathrm{L^{1-}}\right][\mathrm{H^+}]^2} \exp\left[-(1-2)\mathrm{F}\Psi/RT\right] \qquad [26]$$

where F is the Faraday constant, Ψ is the surface potential, R is the molar gas constant, T is the absolute temperature, and square brackets represent concentrations. The exponential terms are correction factors accounting for the effect of surface charge on surface complexation. [20]–[25] are considered in the constant capacitance model where $\Psi = \Psi_\mathrm{o}$. In the diffuse layer model, eqn [25] is replaced with eqn [26] and $\Psi = \Psi_\mathrm{d}$.

Equilibrium constants for outer-sphere surface complexation in the triple layer model are:

$$K_\mathrm{M}^3 = \frac{[\mathrm{SO^- - M^{m+}}][\mathrm{H^+}]}{[\mathrm{SOH}][\mathrm{M^{m+}}]} \exp\left[\mathrm{F}\left(\mathrm{m}\Psi_\beta - \Psi_\mathrm{o}\right)/RT\right] \qquad [27]$$

$$K_\mathrm{M}^4 = \frac{\left[\mathrm{SO^- - MOH^{(m-1)}}\right][\mathrm{H^+}]^2}{[\mathrm{SOH}][\mathrm{M^{m+}}]} \exp\left[\mathrm{F}\left((\mathrm{m}-1)\Psi_\beta - \Psi_\mathrm{o}\right)/RT\right] \qquad [28]$$

$$K_{\mathrm{L}}^{4} = \frac{[\mathrm{SOH_2^+ - L^{1-}}]}{[\mathrm{SOH}][\mathrm{H^+}][\mathrm{L^{1-}}]} \exp\left[\mathrm{F}(\Psi_{\mathrm{o}} - 1\Psi_{\beta})/RT\right] \qquad [29]$$

$$K_{\mathrm{L}}^{5} = \frac{[\mathrm{SOH_2^+ - LH^{(1-1)-}}]}{[\mathrm{SOH}][\mathrm{H^+}]^2[\mathrm{L^{1-}}]} \exp\left[\mathrm{F}(\Psi_{\mathrm{o}} - (1-1)\Psi_{\beta})/RT\right] \qquad [30]$$

$$K_{\mathrm{C}} = \frac{[\mathrm{SO^- - C^+}][\mathrm{H^+}]}{[\mathrm{SOH}][\mathrm{C^+}]} \exp\left[\mathrm{F}(\Psi_{\beta} - \Psi_{\mathrm{o}})/RT\right] \qquad [31]$$

$$K_{\mathrm{A}} = \frac{[\mathrm{SOH_2^+ - A^-}]}{[\mathrm{SOH}][\mathrm{H^+}][\mathrm{A^-}]} \exp\left[\mathrm{F}(\Psi_{\mathrm{o}} - \Psi_{\beta})/RT\right] \qquad [32]$$

In the one-pK model the equilibrium constants for surface complexation are:

$$K_{\mathrm{H}} = \frac{[\mathrm{SOH_2^{1/2+}}]}{[\mathrm{SOH^{1/2-}}][\mathrm{H^+}]} \exp[\mathrm{F}\Psi_{\mathrm{o}}/RT] \qquad [33]$$

$$K_{\mathrm{M}}^{1} = \frac{[\mathrm{SOH^{1/2-} - M^{m+}}]}{[\mathrm{SOH^{1/2-}}][\mathrm{M^{m+}}]} \exp[\mathrm{mF}\Psi_{\mathrm{d}}/RT] \qquad [34]$$

$$K_{\mathrm{M}}^{2} = \frac{[\mathrm{SOH^{1/2-} - MOH^{(m-1)}}][\mathrm{H^+}]}{[\mathrm{SOH^{1/2-}}][\mathrm{M^{m+}}]} \exp[(\mathrm{m}-1)\mathrm{F}\Psi_{\mathrm{d}}/RT] \qquad [35]$$

$$K_{\mathrm{L}} = \frac{[\mathrm{SOH_2^{1/2+} - L^{1-}}]}{[\mathrm{SOH_2^{1/2+}}][\mathrm{L^{1-}}]} \exp[-1\mathrm{F}\Psi_{\mathrm{d}}/RT] \qquad [36]$$

$$K_{\mathrm{C}} = \frac{[\mathrm{SOH^{1/2-} - C^+}]}{[\mathrm{SOH^{1/2-}}][\mathrm{C^+}]} \exp[\mathrm{F}\Psi_{\mathrm{d}}/RT] \qquad [37]$$

$$K_{\mathrm{A}} = \frac{[\mathrm{SOH_2^{1/2+} - A^-}]}{[\mathrm{SOH_2^{1/2+}}][\mathrm{A^-}]} \exp[-\mathrm{F}\Psi_{\mathrm{d}}/RT] \qquad [38]$$

Mass and Charge Balances

The mass balance expression for the surface functional group, SOH, in the two-pK models is:

$$\begin{aligned} S_{\mathrm{T}} = {} & [\mathrm{SOH}] + [\mathrm{SOH_2^+}] + [\mathrm{SO^-}] + [\mathrm{SOM^{(m-1)}}] + 2[\mathrm{(SO)_2M^{(m-2)}}] + [\mathrm{SL^{(1-1)-}}] + 2[\mathrm{S_2L^{(1-2)-}}] + [\mathrm{SHL^{(1-2)-}}] \\ & + [\mathrm{SO^- - M^{m+}}] + [\mathrm{SO^- - MOH^{(m-1)}}] + [\mathrm{SOH_2^+ - L^{1-}}] + [\mathrm{SOH_2^+ - LH^{(1-1)-}}] + [\mathrm{SO^- - C^+}] + [\mathrm{SOH_2^+ - A^-}] \end{aligned} \qquad [39]$$

The mass balance for the surface functional groups, SOH and $\mathrm{SOH_2}$, in the one-pK model is:

$$\begin{aligned} S_{\mathrm{T}} = {} & [\mathrm{SOH^{1/2-}}] + [\mathrm{SOH_2^{1/2+}}] + [\mathrm{SOH^{1/2-} - M^{m+}}] + [\mathrm{SOH^{1/2-} - MOH^{(m-1)}}] + [\mathrm{SOH_2^{1/2+} - L^{1-}}] + [\mathrm{SOH^{1/2-} - C^+}] \\ & + [\mathrm{SOH_2^{1/2+} - A^-}] \end{aligned} \qquad [40]$$

The mass balance represents a summation of all surface species considered in the particular surface complexation model. The charge balance expressions for the two-pK models are:

$$\begin{aligned} \sigma_{\mathrm{o}} = {} & [\mathrm{SOH_2^+}] + [\mathrm{SOH_2^+ - L^{1-}}] + [\mathrm{SOH_2^+ - LH^{(1-1)-}}] + (\mathrm{m}-1)[\mathrm{SOM^{(m-1)}}] + (\mathrm{m}-2)[\mathrm{(SO)_2M^{(m-2)}}] + [\mathrm{SOH_2^+ - A^-}] \\ & - [\mathrm{SO^-}] - [\mathrm{SO^- - M^{m+}}] - [\mathrm{SO^- - MOH^{(m-1)}}] - (1-1)[\mathrm{SL^{(1-1)-}}] - (1-2)[\mathrm{S_2L^{(1-2)-}}] - (1-2)[\mathrm{SHL^{(1-2)-}}] \\ & - [\mathrm{SO^- - C^+}] \end{aligned} \qquad [41]$$

$$\begin{aligned} \sigma_{\beta} = {} & \mathrm{m}[\mathrm{SO^- - M^{m+}}] + (\mathrm{m}-1)[\mathrm{SO^- - MOH^{(m-1)}}] + [\mathrm{SO^- - C^+}] - 1[\mathrm{SOH_2^+ - L^{1-}}] - (1-1)[\mathrm{SOH_2^+ - LH^{(1-1)-}}] \\ & - [\mathrm{SOH_2^+ - A^-}] \end{aligned} \qquad [42]$$

$$\sigma_{\mathrm{o}} + \sigma_{\beta} + \sigma_{\mathrm{d}} = 0 \qquad [43a]$$

$$\sigma_{\mathrm{o}} + \sigma_{\mathrm{d}} = 0 \qquad [43b]$$

where σ is the surface charge. The charge balances, [41] and [42], represent the summation of all charge contributions in a particular plane of adsorption. All of the models consider charge balance in the surface plane, eqn [41]. Charge balance in the β-plane, eqn [42], is restricted to the triple-layer model. Charge balance eqn [43a] is considered in the triple-layer model while eqn [43b] is used in the diffuse-layer model. The charge balance expressions for the one-pK model based on the Stern model are eqn [43b] and:

$$\sigma_{\mathrm{o}} = \frac{1}{2}\left(\left[\mathrm{SOH}_2^{1/2+}\right] - \left[\mathrm{SOH}^{1/2-}\right]\right) \qquad [44]$$

Charge-Potential Relationships

All surface complexation models contain relations between surface charges and surface potentials. In the constant capacitance model the charge-potential relationship is:

$$\sigma = C\Psi \qquad [45]$$

where C is the capacitance. The charge potential relationship for the diffuse layer model is:

$$\sigma_{\mathrm{d}} = -(8\varepsilon_{\mathrm{o}} DRTI)^{1/2} \sinh\left(\mathrm{F}\Psi_{\mathrm{d}}/2RT\right) \qquad [46]$$

where ε_{o} is the permittivity of vacuum, D is the dielectric constant of water, and I is the solution ionic strength. In the triple-layer model the charge potential relationships are eqn [46] and:

$$\sigma_{\mathrm{o}} = C_1\left(\Psi_{\mathrm{o}} - \Psi_{\beta}\right) \qquad [47]$$

$$\sigma_{\mathrm{d}} = C_2\left(\Psi_{\mathrm{d}} - \Psi_{\beta}\right) \qquad [48]$$

The charge-potential relationships for the one-pK model based on the Stern model are eqn [46] and:

$$\sigma_{\mathrm{o}} = C(\Psi_{\mathrm{o}} - \Psi_{\mathrm{d}}) \qquad [49]$$

Obtaining Values of Adjustable Parameters

Surface Site Density

The total number of reactive surface functional groups, S_{T} is an important adjustable parameter in the surface complexation models and is related to the surface site density:

$$S_{\mathrm{T}} = \frac{Sa10^{18}}{\mathrm{N_A}} N_{\mathrm{S}} \qquad [50]$$

where S is the surface area, a is the particle concentration, and $\mathrm{N_A}$ is Avogadro's number. Experimental methods for determining surface site density include: tritium exchange, potentiometric titration, fluoride adsorption, and maximum adsorption. Values of this parameter can also be calculated from crystal dimensions or optimized to fit experimental adsorption data. Various determinations of surface site density vary by an order of magnitude; the lowest values are obtained from crystallographic calculations while tritium exchange yields the highest values. Uncertainty in the value of the surface site density is a major limitation in the use of surface complexation models since the ability of the models to describe adsorption is sensitively dependent on this value. To standardize surface complexation modeling, a fixed value of 2.31 sites nm^{-2} has been used for many natural materials. Applications of the diffuse-layer model to metal adsorption have split the total number of reactive surface functional groups into a 'strong,' S_{s}, and a 'weak,' S_{w}, set of adsorption sites. This approach greatly increases the number of adjustable parameters since each set of sites, S_{i}, has its own protonation, dissociation, and metal surface complexation constants.

Capacitances

Some values of capacitance (C in the constant capacitance and one-pK model and C_1 in the triple layer model) can be obtained graphically from slopes of protonation-dissociation constants versus surface charge. Alternatively, both capacitances, C_1 and C_2, in the triple-layer model can be obtained using an electrokinetic extrapolation technique. Capacitance values obtained experimentally usually exhibit great variability; therefore, capacitances have generally been optimized to fit the titration data.

Surface Complexation Constants

Values of the protonation and dissociation constants in the constant capacitance model and the triple-layer model can be obtained from the same graphs used to obtain values of capacitance. These constants can also be obtained by optimizing titration data using a computer program. Values of the surface complexation constants for ion adsorption are obtained using computer optimization. An advantage of computer optimization, in addition to ease of use, is that it yields bias-free parameters with standard deviations and quality-of-fit criteria. Individual optimized equilibrium constant values can be weighted to obtain overall best estimates of the parameter:

$$\overline{\log K} = \sum \frac{(1/\sigma_{\log \mathrm{K}})_i}{\sum (1/\sigma_{\log \mathrm{K}})_i} [\log K]_i \qquad [51]$$

For the diffuse layer model a set of best estimates of log*K* are available for a variety of adsorbing cations and anions. The advantage of this data set is that the surface complexation constants are all self-consistent; i.e., all ion surface complexation constants were optimized using the same values of protonation-dissociation constants and surface site density. This is an important point since parameter values in the surface complexation models are interdependent. Additionally, since each surface complexation model contains a different set of assumptions for the solid–solution interface, surface complexation constants from one model must not be used in any other model.

Applications to Ion Adsorption on Natural Samples

All surface complexation models were originally developed to describe charging behavior and ion adsorption of ions on oxide minerals. Various curves are commonly used to describe adsorption behavior: adsorption isotherms, adsorption edges, and adsorption envelopes. Adsorption isotherms describe ion adsorption as a function of equilibrium ion concentration, usually at fixed solution pH. Adsorption edges and adsorption envelopes both describe ion adsorption as a function of solution pH at a fixed total ion concentration. Adsorption edge is the term generally applied to cation adsorption, while the term adsorption envelope is used to describe anion adsorption.

The most commonly studied oxide surfaces with surface complexation models have been the iron oxides goethite and ferrihydrite. Subsequently, the models were extended to include adsorption on clay minerals, organic materials, and soil samples. In extending the models to natural samples certain approximations and modifications are necessary. In the application to natural systems, such as clay minerals or soils, the assumption is made that ion adsorption occurs through interaction with the hydroxyl groups at the edges of the clay particles. The effect of permanent negatively charged sites at the clay basal planes on this adsorption process is ignored. This simplification may not be appropriate, especially for anions whose edge adsorption may be affected by this negative charge.

The surface complexation models contain the assumption that ion adsorption takes place on one or at most two sets of reactive surface sites. This is clearly an oversimplification since even simple oxide minerals contain several sets of reactive hydroxyl groups. However, this simplification is necessary to maintain the number of adjustable parameters at a reasonable level. Natural materials such as soils are complex, multisite mixtures having a variety of reactive surface functional groups. Thus surface complexation constants determined for soils represent average composite values for all these sets of reactive surface functional groups.

Constant Capacitance Model

The constant capacitance model has been used to describe adsorption on silicon, aluminum, iron, and titanium oxides, kaolinite, montmorillonite, and illite clay minerals, plant cell walls, sediments, and soils. Adsorbing ions that have been investigated include the cation and metal ions: calcium, cesium, lead, copper, cadmium, zinc, nickel, cobalt, aluminum, iron, manganese, silver, mercury, lanthanum, europium, ytterbium, and the anions: phosphate, sulfate, arsenate, arsenite, selenite, selenate, borate, molybdate, silicate, fluoride, phthalate, salicylate, benzoate, citrate.

Examples of the fit of the constant capacitance model to trace metal adsorption edges are provided in Figure 2 for iron, lead, copper, and cadmium adsorption on silica. As for many trace metal cations, the amount of adsorption increases rapidly from 0 to 100% over a narrow pH range. The model is well able to describe these changes in adsorption for the four different metal ions. Figure 3 indicates the ability of the constant capacitance model to fit adsorption envelopes for the anion, silicate, on to the iron oxide, goethite at various initial silicate concentrations. Silicate adsorption is nearly constant over most of the pH range. The model is able to describe the adsorption, including the pH dependence observed at the highest initial silicate concentration.

Applications of the constant capacitance model to soils have been restricted to anions: phosphate, arsenate, selenite, borate, and molybdate. For the application of the model to selenite adsorption by soils, two sets of reactive surface functional groups were postulated; monodentate surface complexes were formed on one set of sites and bidentate surface complexes on the other. The model was initially applied to one Californian soil. As can be seen in Figure 4(a), the fit of the model to the data is good. Subsequently, the model parameters obtained in fitting this soil were used to predict adsorption on additional Californian soils. Figure 4(b) shows that this prediction was qualitatively successful and indicates some predictive capability of the model for soils of somewhat similar chemical and physical characteristics.

An alternative approach has been developed for describing borate adsorption on soils. From the fitted surface complexation constants for a set of soils, a general regression model was obtained that predicts the surface complexation constants for new soils from easily measured chemical parameters: surface area, organic carbon content, inorganic carbon content, and aluminum oxide

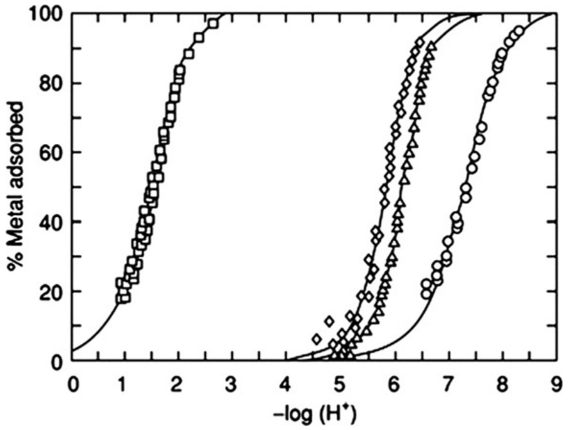

Figure 2 Fit of the constant capacitance model to metal adsorption on silica. Model results are represented by solid lines. □ Fe; ◇ Pb; △ Cu; ○ Cd. Reprinted with permission from Schindler, P.W., Fürst, B., Dick, R., and Wolf, P.U. (1976). Ligand properties of surface silanol groups, I. Surface complex formation with Fe^{3+}, Cu^{2+}, Cd^{2+}, and Pb^{2+}. *Journal of Colloid Interface Science* 55, 469–475.

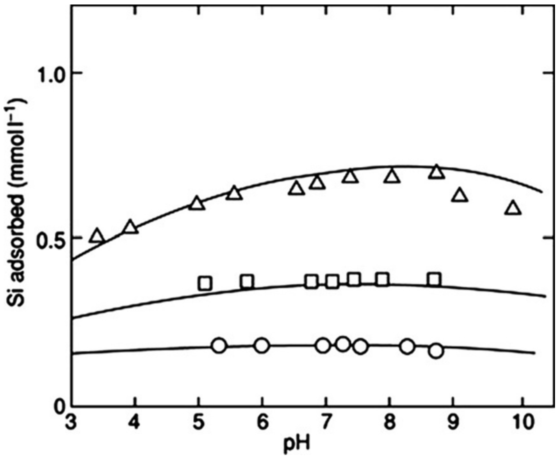

Figure 3 Fit of the constant capacitance model to silicate adsorption on goethite. Model results are represented by solid lines. ○ 2×10^{-4} M; □ 4×10^{-4} M; △ 8×10^{-4} M. Reprinted from Sigg, L.M. and Stumm, W. (1981). The interaction of anions and weak acids with the hydrous goethite (α-FeOOH) surface. In: *Colloids and Surfaces*, vol. 2, pp. 101–117. Amsterdam: Elsevier Science.

content. These surface complexation constants were then used in the constant capacitance model to predict borate adsorption on the new soils. This approach constitutes a completely independent model evaluation that was able to predict borate adsorption on a diverse set of soils having a wide range of chemical properties, as indicated in Figure 5.

This soil approach was also used successfully to predict molybdate adsorption from the chemical properties: cation exchange capacity, organic and inorganic carbon content, and iron oxide content as well as arsenate and selenite adsorption using five soil chemical properties.

Diffuse-Layer Model

The diffuse-layer model has been used to describe adsorption on iron, aluminum, manganese, titanium, and silicon oxides, kaolinite, montmorillonite and biotite minerals, natural organic matter, bacterial cell walls, and sediments. Adsorbing ions that have been investigated include the cation and metal ions: calcium, strontium, barium, copper, nickel, zinc, cadmium, lead, cobalt, aluminum, chromium, silver, mercury, uranium and the anions: phosphate, sulfate, selenite, selenate, arsenate, arsenite, borate, chromate, fluoride, vanadate, thiosulfate, oxalate, phthalate, salicylate, benzoate, and fulvate.

The ability of the diffuse-layer model to describe metal adsorption edges is indicated in Figure 6 for lead adsorption on the iron oxide, hematite. The model was able to describe the data very well at three significantly different initial lead concentrations over a wide range of solution pH values. Figure 7 demonstrates the ability of the diffuse-layer model to fit adsorption envelopes for the chromate anion on goethite. In order to fit the two intermediate chromate concentrations it was necessary to add a

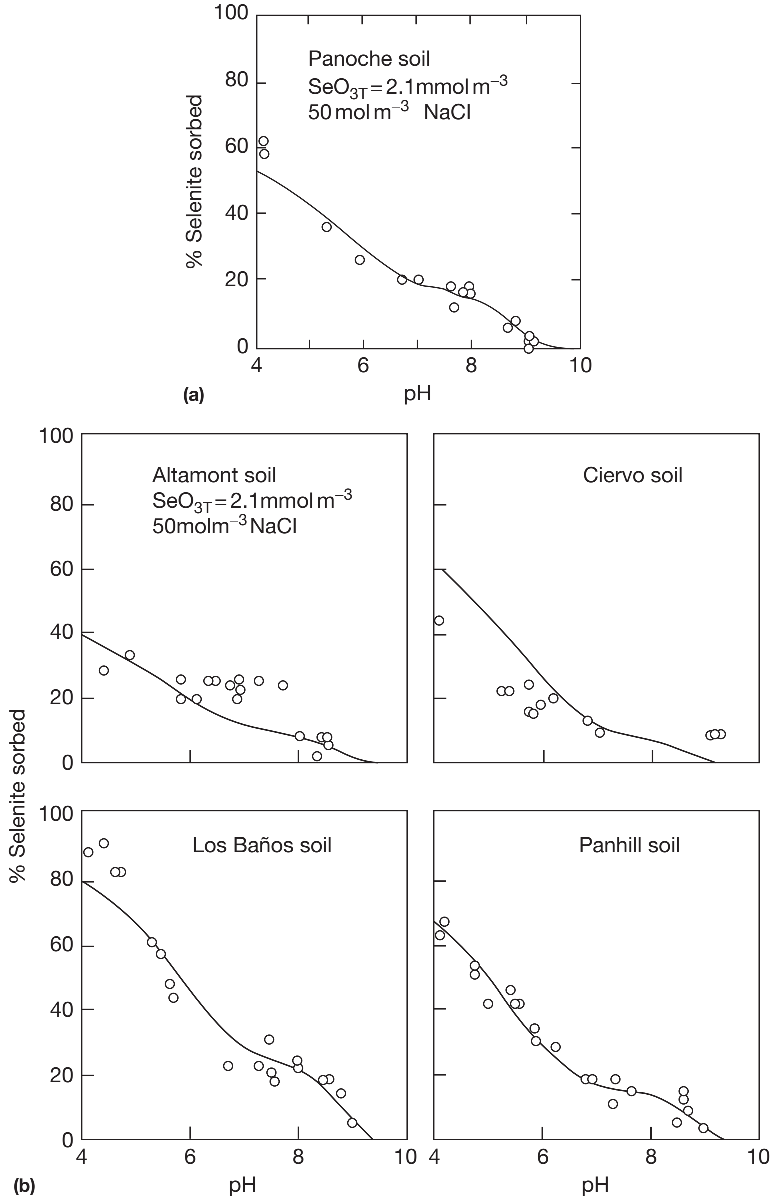

Figure 4 (a) Fit of the constant capacitance model to selenite adsorption on a California soil. Model fit is represented by a solid line. (b) Constant capacitance model predictions of selenite adsorption by California soils. Model predictions are represented by solid lines. Reprinted with permission from Sposito, G., de Wit, J.C.M., and Neal, R.H. (1988). Selenite adsorption on alluvial soils: III. Chemical modeling. *Soil Science Society of America Journal* 52, 947–950.

third chromate surface complex, $[SCrO_4^{3-}]$. With this addition, the model is well able to describe chromate adsorption at all initial chromate concentrations over a wide range of solution pH.

Adsorption of various metal ions has been investigated on a lignocellulose organic substrate extracted from wheat bran. In these applications, two sets of reactive surface functional groups are considered representing carboxylic and phenolic sites. Figure 8 presents the ability of the diffuse-layer model to describe copper adsorption edges on this organic material as a function of initial copper concentration $[Cu_{ini}]$, solution pH, and ionic strength, I. In this application, the model is fitted to the data for $[Cu_{ini}] = 2 \times 10^{-4}$ M, $I = 0.1$. The model parameters resulting from this optimization were then used to predict the remaining model results depicted in Figure 8. The diffuse layer model is well able to describe copper adsorption on this natural material.

The diffuse layer model has been used to describe arsenic adsorption by a contaminated soil profile. In this application it was assumed that amorphous iron oxide was the principal reactive adsorbent. The modeling was successful in describing arsenic adsorption in the two layers containing the most extractable iron.

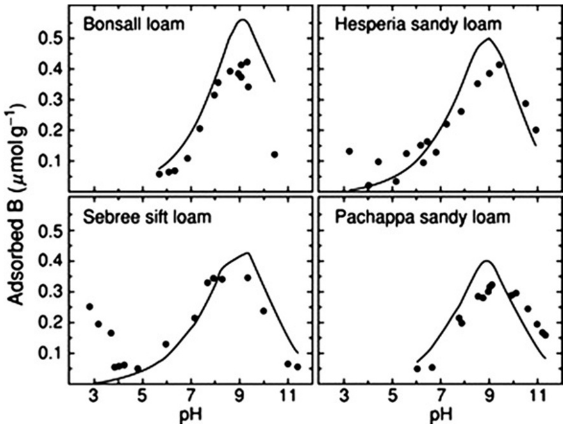

Figure 5 Constant capacitance model predictions of boron adsorption by soils of various soil chemical properties and diverse soil orders. Model predictions are represented by solid lines. Modified from Goldberg, S., Lesch, S.M., and Suarez, D.L. (2000). Predicting boron adsorption by soils using soil chemical parameters in the constant capacitance model. *Soil Science of Society of America Journal* 64, 1356–1363.

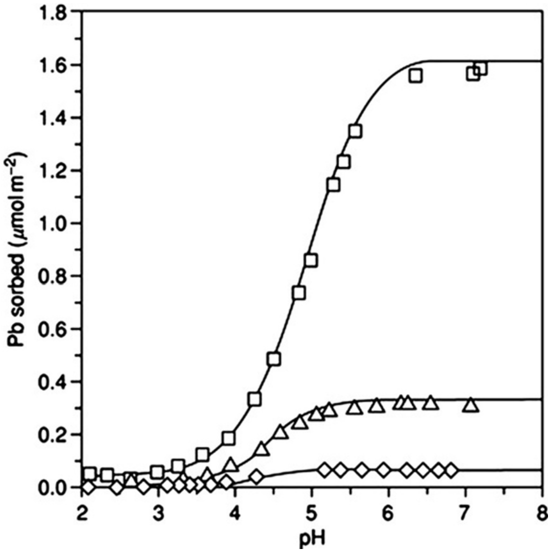

Figure 6 Fit of the diffuse layer model to lead adsorption on hematite. Model fits are represented by solid lines. □ 100 μmol l^{-1}; △ 20 μmol l^{-1}; ◇ 4 μmol l^{-1}. Reproduced with permission from Christl, D.I. and Kretzschmar, R. (1999). Competitive sorption of copper and lead at the oxide–water interface: implications for surface site density. *Geochimica et Cosmochimica Acta* 63, 2929–2938.

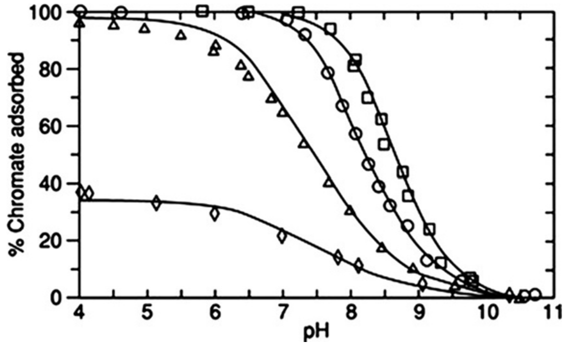

Figure 7 Fit of the diffuse layer model to chromate adsorption on goethite. Model fits are represented by solid lines. □ 0.01 mmol l^{-1}; ○ 0.05mmol l^{-1}; △ 0.2mmol l^{-1}; ◇ 0.8 mmol l^{-1}. Reprinted with permission from Mesuere, K. and Fish, W. (1992). Chromate and oxalate adsorption on goethite: I. Calibration of surface complexation models. *Environmental Science and Technology* 26, 2357–2364. Copyright American Chemical Society.

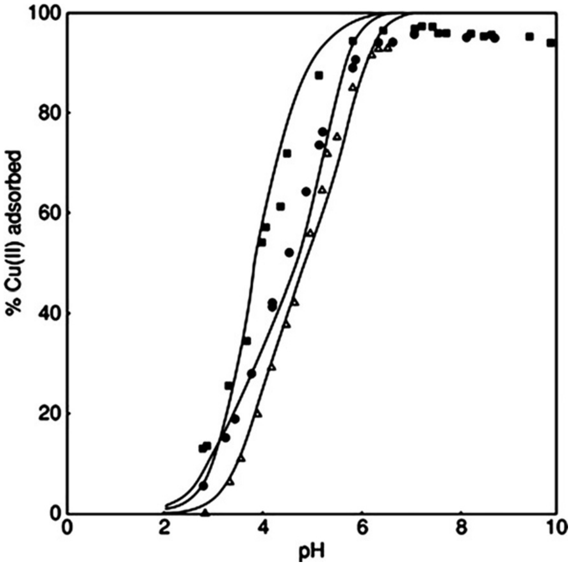

Figure 8 Fit of the diffuse layer model to copper adsorption on lignocellulose extracted from wheat bran. Model fits are represented by solid lines. △ $[Cu(II)]_{ini}=2.10^{-4}$ mol l^{-1}, I = 0.1; ● $[Cu(II)]_{ini}=2.10^{-4}$ mol l^{-1}, I = 0.01; ▪ $[Cu(II)]_{ini}=2.10^{-5}$ mol l^{-1}, I = 0.1. Reproduced with permission from Ravat, C., Dumonceau, J., and Monteil-Rivera, F. (2000). Acid/base and Cu(II) binding properties of natural organic matter extracted from wheat bran: modeling by the surface complexation model. *Water Research* 34, 1327–1329.

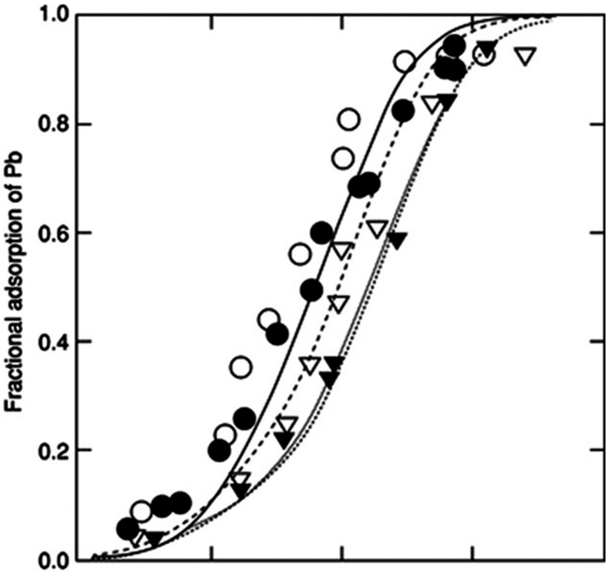

Figure 9 Fit of the triple-layer model to lead adsorption on goethite. Model fits are represented by solid lines. ○ 9.65 μmol l^{-1}; ● 24.1 μmol l^{-1}; ▽ 48.3 μmol l^{-1}; ▼ 72.4 μmol l^{-1}. Reproduced with permission from Kooner, Z.S., Cox, C.D., and Smoot, J.L. (1995). Prediction of adsorption of divalent heavy metals at the goethite/water interface by surface complexation modeling. *Environmental Toxicology and Chemistry* 14, 2077–2083. Copyright SETAC, Pensacola, Florida, USA.

Triple-Layer Model

The triple-layer model has been used to describe adsorption on iron, aluminum, manganese, and silicon oxides, kaolinite and smectite clay minerals, and soils. Adsorbing ions that have been investigated include the cation and metal ions: sodium, potassium, calcium, magnesium, lead, zinc, cadmium, copper, cobalt, silver, mercury, uranium, plutonium, thorium, neptunium, and the anions: chloride, nitrate, perchlorate, sulfate, selenite, selenate, arsenate, arsenite, molybdate, borate, chromate, silicate, fluoride, carbonate, oxalate, phthalate, salicylate, lactate, acetate, formate, and humate.

The ability of the triple-layer model to describe metal ion adsorption edges is depicted in Figure 9 for lead adsorption on goethite. In this application an inner-sphere surface complex is assumed. The triple-layer model was well able to describe lead

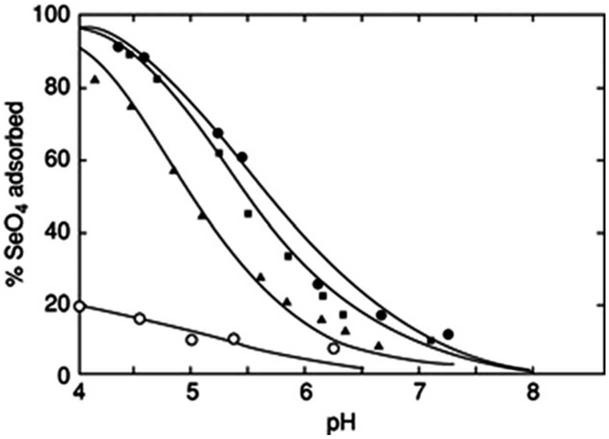

Figure 10 Fit of the triple-layer model to selenate adsorption on amorphous iron oxide. Model fits are represented by solid lines. Total SeO$_4$ added ● 2×10^{-7} mol l^{-1}; ▪ 2×10^{-5} mol l^{-1}; ▲ 2×10^{-4} mol l^{-1}; ○ 2×10^{-3} mol l^{-1}. Reproduced with permission from Davis, J.A. and Leckie, J.O. (1980). Surface ionization and complexation at the oxide/water interface. III. Adsorption of anions. *Journal of Colloid Interface Science* 74, 32–43.

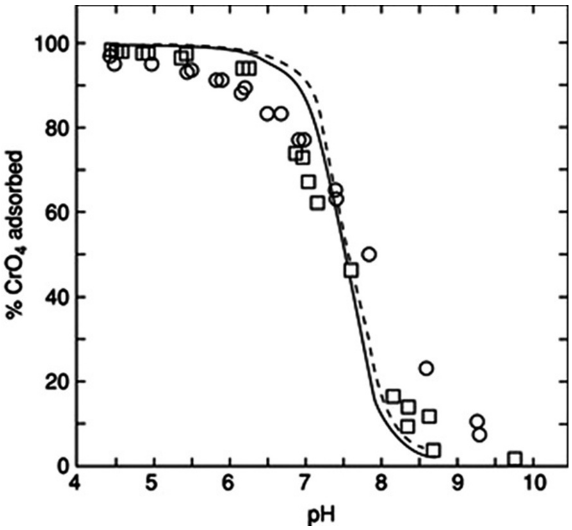

Figure 11 Fit of the triple-layer model to chromate adsorption on two soils. Model fits are represented by solid lines. □ Holston/Cloudland series soil; ○ Cecil/Pacolet series soil. Reprinted with permission from Zachara, J.M., Ainsworth, C.C., Cowan, C.E., and Resch, C.T. (1989). Adsorption of chromate by subsurface soil horizons. *Soil Science of America Journal* 53, 418–428.

adsorption at various initial concentrations as a function of solution pH. Figure 10 shows the fit of the triple-layer model to anion adsorption envelopes for selenate adsorption on the iron oxide, ferrihydrite. With the assumption of two outer-sphere surface complexes, the model describes the adsorption data quantitatively for four vastly differing initial selenium concentrations as a function of solution pH.

The triple-layer model was able to fit calcium, magnesium, and sulfate adsorption on a Brazilian oxisol and sulfate adsorption on an acidic forest soil. Molybdate adsorption on two Californian soils as a function of solution pH and ionic strength could be described using either an inner-sphere or an outer-sphere adsorption mechanism. The quality of the fit was slightly better with the inner-sphere adsorption mechanism. In this application it was assumed that aluminol groups on the clay edges are the reactive surface functional groups in the soils and that surface complexation constants determined for reactive surface hydroxyls of aluminum oxide can be used to describe the surface complexation reactions undergone by these aluminol groups.

In a similar approach, surface complexation constants previously determined for the reactions undergone by aluminum-substituted goethite were used to describe chromate adsorption by two soils. It was assumed that only the iron sites on the aluminum-substituted goethite are involved in chromate adsorption, forming monodentate outer-sphere surface complexes. The ability of the model to describe chromate adsorption on the two soils as a function of solution pH is indicated in Figure 11. The fit of the model on these heterogeneous materials is qualitatively correct.

The general regression model prediction equation approach was incorporated into the triple layer model and used to describe molybdate adsorption by soils. Using both an inner-sphere and an outer-sphere surface configuration the model prediction of molybdenum adsorption was improved over that obtained using the constant capacitance model, especially at high solution pH.

One-pK Model

The one-pK model has been used to describe adsorption on iron, aluminum, and titanium oxides. The vast majority of studies to date have used goethite as the adsorbent material. Adsorbing ions that have been investigated include the cations: potassium, calcium, cadmium, copper, and anions: phosphate, arsenate, selenite, sulfate, chromate, lactate, oxalate, malonate, phthalate, citrate, and fulvate.

The ability of the Stern model based one-pK model to fit cation adsorption isotherms is indicated in Figure 12 for cadmium adsorption on hematite. The model was well able to describe cadmium adsorption at various solution pH values and initial cadmium concentrations. In this application, consideration of background electrolyte surface complexes was neglected. Figure 13 indicates the ability of the Stern model based one-pK model to fit anion adsorption isotherms for phosphate adsorption on goethite. The model was well able to describe phosphate adsorption over a very wide range of solution pH values and initial phosphate concentrations. In this application, a surface complexation constant for potassium adsorption was also optimized.

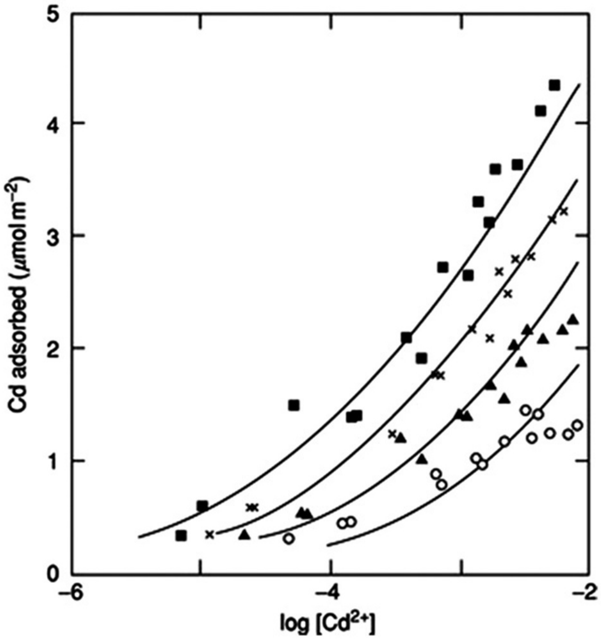

Figure 12 Fit of the one-pK model to cadmium adsorption on amorphous iron oxide. Model fits are represented by solid lines. pH ○ 7.0; ▲ 7.4; × 7.7; ▪ 8.0. Reproduced with permission from van Riemsdijk, W.H., de Wit, J.C.M., Koopal, L.K., and Bolt, G.H. (1987). Metal adsorption on heterogeneous surfaces: adsorption models. *Journal of Colloid Interface Science* 116, 511–522.

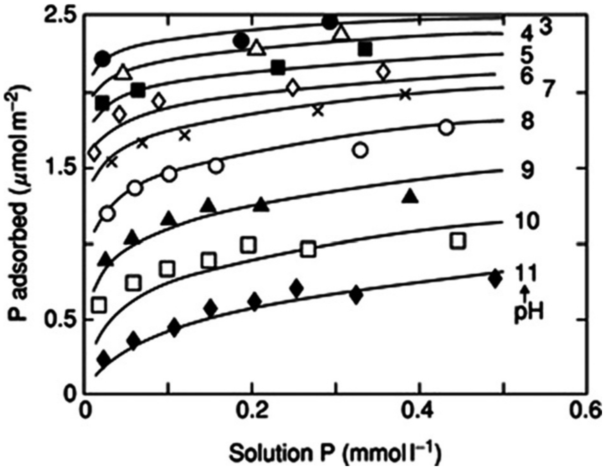

Figure 13 Fit of the one-pK model to phosphate adsorption on goethite. Model fits are represented by solid lines. Reproduced with permission from van Riemsdijk, W.H. and van der Zee S.E.A.T.M. (1991). Comparisons of Models for Adsorption, Solid Solution and Surface Precipitation (based on experimental data of Bowden et al. (1980)). In: Bolt, G.H. et al. (eds) *Interactions at the Soil Colloid–Soil Solution Interface*, pp. 241–256. Dordrecht, The Netherlands: Kluwer.

The CD-MUSIC model was able to describe adsorption by a soil dominant in ferrihydrite and allophane over most of the range of arsenic concentrations studied. Because many parameters were fit, considerable uncertainty exists in regard to the uniqueness of the mathematical solution.

Further Reading

Bolt GH and van Riemsdijk WH (1982) Ion adsorption on inorganic variable charge constituents. In: Bolt GH (ed.) *Soil chemistry, part B. Physicochemical methods*, pp. 459–503. Amsterdam: Elsevier.

Davis JA and Kent DB (1990) Surface complexation modeling in aqueous geochemistry. *Reviews in Mineralogy* 23: 177–260.

Dzombak DA and Morel FMM (1990) *Surface complexation modeling. Hydrous ferric oxide*. New York: John Wiley.

Goldberg S (1992) Use of surface complexation models in soil chemical systems. *Advances in Agronomy* 47: 233–329.

Goldberg S (1993) Constant capacitance model: chemical surface complexation model for describing adsorption of toxic trace elements on soil minerals. *American Chemical Society Symposium Series* 518: 278–307.

Goldberg S (1995) Adsorption models incorporated into chemical equilibrium models. In: Loeppert R, Schwab AP, and Goldberg S (eds.) *Chemical equilibrium and reaction models*, pp. 37–60. Madison: Soil Science Society of America.

Goldberg S (1998) Ion adsorption at the soil particle-solution interface: Modeling and mechanisms. In: Huang PM, Senesi N, and Buffle J (eds.) IUPAC Series on analytical and physical chemistry of environmental systems. *Structure and surface reactions of soil particles*, 4, pp. 377–412. Chichester: Wiley.

Goldberg S and Criscenti LJ (2008) Modeling adsorption of metals and metalloids by soil components. In: Violante A, Huang PM, and Gadd GM (eds.) *Biophysico-chemical processes of heavy metals and metalloids in soil environments*, pp. 215–264. Hoboken: Wiley.

Hiemstra T and van Riemsdijk WH (2002) On the relationship between surface structure and ion complexation of oxide-solution interfaces. In: Hubbard AT (ed.) *Encyclopedia of surface and colloid science*, pp. 3773–3799. New York: Marcel Dekker.

James RO and Parks GA (1982) Characterization of aqueous colloids by their electrical double-layer and intrinsic surface chemical properties. *Surface and Colloid Science* 12: 1119–1216.

Sposito G (1983) Foundations of surface complexation models of the oxide–aqueous solution interface. *Journal of Colloid and Interface Science* 91: 329–340.

Sposito G (1984) *The surface chemistry of soils*. Oxford: Oxford University Press.